Treatments with the specific δ-secretase inhibitor, compound 11, promote the regeneration of motor and sensory axons after peripheral nerve injury.

Robin Isaacson[1], Dario Carrasco[1], Hannah Holliday[1], Seong Kang[1], Samia Khan[1], David Kim[1], Xia Liu[1], Keqiang Ye[2], and Arthur English[1]

[1]Emory University School of Medicine
[2]Shenzhen Institutes of Advanced Technology Chinese Academy of Sciences

June 1, 2023

Abstract

Limited axon regeneration following peripheral nerve injury may be related to activation of the lysosomal protease, asparaginyl endopeptidase (AEP, δ-secretase), and its degradation of the microtubule associated protein, Tau. Activity of AEP was increased at the site of sciatic nerve transection and repair but blocked in mice treated systemically with a specific AEP inhibitor, compound 11 (CP11). Treatments with CP11 enhanced axon regeneration in vivo. Amplitudes of compound muscle action potentials recorded four weeks after nerve transection and repair and two weeks after daily treatments with CP11 were double those of vehicle-treated mice. At that time after injury, axons of significantly more motor and sensory neurons had regenerated successfully and reinnervated the tibialis anterior and gastrocnemius muscles in CP11-treated mice than vehicle-treated controls. In cultured adult dorsal root ganglion neurons derived from wild type mice that were treated in vitro for 24 hours with CP11, neurites were nearly 50% longer than in vehicle-treated controls, and similar to neurite lengths in cultures treated with the TrkB agonist, 7,8-dihydroxyflavone (7,8-DHF). Combined treatment with CP11 and 7,8-DHF did not enhance outgrowth more than treatments with either one alone. Enhanced neurite outgrowth produced by CP11 was found also in the presence of the TrkB inhibitor, ANA-12, indicating that the enhancement was independent of TrkB signaling. Longer neurites were found after CP11 treatment in both TrkB+ and TrkB- neurons. Delta secretase inhibition by CP11 is a treatment for peripheral nerve injury with great potential.

Treatments with the specific δ-secretase inhibitor, compound 11, promote the regeneration of motor and sensory axons after peripheral nerve injury.

Robin H. Isaacson[1], Dario I. Carrasco[1], Hannah Holliday[1], Seong Su Kang[2], Samia Khan[1], David Kim[1], Xia Liu[2], Keqiang Ye[3], and Arthur W. English[1]

Departments of Cell Biology[1] and Pathology & Laboratory Medicine[2], Emory University School of Medicine, Atlanta, GA, USA

and

Faculty of Life and Health Sciences, and Brain Cognition and Brain Disease Institute (BCBDI), Shenzhen Institute of Advanced Technology (SIAT), Chinese Academy of Sciences, Shenzhen, Guangdong 518055, China[3]

Running title : Compound 11 and axon regeneration

Τρεατμεντς ωιτη τηε σπεςιφις δ-σεςρεταση ινηιβιτορ, ςομπουνδ 11, προμοτε τηε ρεγενερατιον οφ μοτορ ανδ σενσορψ αξονς αφτερ περιπηεραλ νερε ινθυρψ.

Abstract

Limited axon regeneration following peripheral nerve injury may be related to activation of the lysosomal protease, asparaginyl endopeptidase (AEP, δ-secretase), and its degradation of the microtubule associated protein, Tau. Activity of AEP was increased at the site of sciatic nerve transection and repair but blocked in mice treated systemically with a specific AEP inhibitor, compound 11 (CP11). Treatments with CP11 enhanced axon regeneration *in vivo* . Amplitudes of compound muscle action potentials recorded four weeks after nerve transection and repair and two weeks after daily treatments with CP11 were double those of vehicle-treated mice. At that time after injury, axons of significantly more motor and sensory neurons had regenerated successfully and reinnervated the tibialis anterior and gastrocnemius muscles in CP11-treated mice than vehicle-treated controls. In cultured adult dorsal root ganglion neurons derived from wild type mice that were treated *in vitro* for 24 hours with CP11, neurites were nearly 50% longer than in vehicle-treated controls, and similar to neurite lengths in cultures treated with the TrkB agonist, 7,8-dihydroxyflavone (7,8-DHF). Combined treatment with CP11 and 7,8-DHF did not enhance outgrowth more than treatments with either one alone. Enhanced neurite outgrowth produced by CP11 was found also in the presence of the TrkB inhibitor, ANA-12, indicating that the enhancement was independent of TrkB signaling. Longer neurites were found after CP11 treatment in both TrkB+ and TrkB- neurons. Delta secretase inhibition by CP11 is a treatment for peripheral nerve injury with great potential.

Acknowledgements

This study was conducted with support from grant NS105982 from the USPHS. The authors have no conflicts of interest to declare.

Data Availability: All data are available on FigShare.com

Key words: axon regeneration, nerve injury, delta secretase, muscle, dorsal root ganglion neurons

Introduction

Following a peripheral nerve injury (PNI), both sensory and motor axons are capable of considerable regeneration. However, functional recovery in nerve-injured patients remains very poor (Scholz *et al.* , 2009; Bekelis *et al.* , 2015). There is general agreement that the source of this poor recovery is the slow and often inefficient process of axon regeneration. Thus, experimental treatments for PNI have largely aimed at enhancing axon regeneration. The most effective of these treatments in pre-clinical studies have been those that increase the activity of injured neurons, such as exercise (Udina *et al.* , 2011a; Udina*et al.* , 2011b; Boeltz *et al.* , 2013; English *et al.* , 2014; Gordon & English, 2016) or low frequency electrical stimulation (ES) (Al-Majed *et al.* , 2000b; Al-Majed *et al.* , 2004). The success of these approaches has been tied to an increase in the binding of brain derived neurotrophic factor (BDNF) to its high affinity tropomyosin related kinase (TrkB) receptor in the regenerating axons (Al-Majed *et al.* , 2000a; Wilhelm *et al.* , 2012). Indeed, systemic treatments with small molecule TrkB agonists (English *et al.* , 2013) or prodrugs that generate them (English *et al.* , 2022) largely recapitulate the success of the activity-dependent therapies.

Asparaginyl endopeptidase (AEP, also known as δ-secretase or legumain), a lysosomal protease implicated in the pathological features of Alzheimer's disease (AD) (Zhang *et al.* , 2014; Zhang *et al.* , 2015), increases rapidly and persistently at the site of nerve injury. There it degrades the axonal microtubule associated protein, Tau, as well as amyloid precursor protein (APP) (English *et al.* , 2021). In mice treated with one hour of ES following sciatic nerve transection and repair, this degradation of Tau and APP is reduced, implying that the success of ES in promoting axon regeneration might be due to an effect on AEP. In mice null for AEP, axon regeneration after peripheral nerve injury is enhanced markedly and regeneration is not further enhanced by treatment with ES (English *et al.* , 2021). Thus, inhibition of AEP might be the principal mechanism by which activity-dependent therapies like ES or exercise enhance regeneration. Treatments that produce a direct inhibition of AEP after nerve injury might be a suitable test of this hypothesis.

In the present study, we used a specific AEP inhibitor, compound 11 (CP11) to evaluate this hypothesis.

It was developed using high-throughput screening as a potential treatment for AD (Zhang*et al.* , 2017). In mouse models of AD, oral treatments with CP11 dramatically reduced Tau fragmentation and blocked the formation of Aβ from APP, both of which are products of AEP activity. We show here that*in vivo* systemic treatments with CP11 reduce AEP enzymatic activity at the site of nerve injury and promote the successful regeneration of motor and sensory axons after PNI. Using primary cultures of adult dorsal root ganglion neurons, we show further that treatments with CP11 result in a marked increase in the extension of neurites that is TrkB-independent.

Methods

Animals and surgical methods – All surgical methods were approved by the Institutional Animal Care and Use Committee of Emory University (Protocol No. PROTO201800101). Adult C57B6/J mice of both sexes were used. These animals were considered wild type (WT). Transection and repair of the sciatic nerve was performed as described previously (Akhter *et al.* , 2019). Briefly, in isoflurane-anesthetized animals, the sciatic nerve was exposed in the thigh, cut and immediately repaired by end-to-end anastomosis, and secured in place using fibrin glue. The glue was prepared at the time of surgery from fibrinogen and thrombin (Akhter *et al.* , 2019) and nothing was added to the glue. All incisions were then closed and the mice returned to their cages. On the third day following surgery, the mice began daily treatments, five days per week for two weeks, either with CP11 (Santa Cruz Biotechnology, catalog # sc-319780) (10 mg/kg) or vehicle (4% DMSO in sesame oil). In one set of experiments (12 mice: six CP11-treated and six vehicle-treated, three males and three females in each treatment group) treatments were administered via intraperitoneal injection. In an additional cohort of eight mice, the CP11 or vehicle treatments were given orally. Doses administered were chosen based on published results (Zhang *et al.* , 2017).

Measurement of AEP enzymatic activity – Under isoflurane anesthesia, sciatic nerves were cut and repaired in WT mice, as described above. Beginning on the third post-operative day, mice were given either CP11 (10mg/kg) or vehicle, orally, each day. One group of animals was euthanized with Euthasol® solution (pentobarbital sodium and phenytoin sodium, 150 mg/Kg) three days after the initial treatment. A second set of animals were euthanized after seven days of treatments. The cut and repaired nerves were harvested, including 1 mm proximal and distal to the injury site. Nerves were harvested from a third group of intact mice that served as a control.

The AEP activity assay used was a modification of one previously described (Wang *et al.* , 2018). Freshly made nerve tissue homogenates (25 μg) in Lysis buffer (50 mM Tris·HCl,pH 7.5, 150 mM NaCl, 1% Nonidet P-40, 5 mM EDTA, 5 mM EGTA, 15 mM MgCl2, 60 mM β-glycerophosphate, 0.1 mM sodium orthovanadate, 0.1 mM NaF, 0.1 mM benzamide, 10 mg/mL aprotinin, 10 mg/mL leupeptin, and 1 mM PMSF) were prepared and incubated with 100 μL reaction buffer (50 mM Sodium Citrated, 0.1% CHAPS, and 1 mM DTT, pH 6.0) containing 10 μM AEP substrate, Z-Ala-Ala-Asn-AMC (Bachem). The AMC released by AEP-mediated substrate cleavage was quantified at 360/460 nm in a fluorescence plate reader at 37 °C in kinetic mode. For quantification, densitometry readings were scaled to the maximum value of all of the specimens tested.

Recording of compound muscle action potentials (M responses) – Four weeks after sciatic nerve transection and repair, and two weeks after the end of treatments, the success of motor axon regeneration and reinnervation to the tibialis anterior (TA) and lateral gastrocnemius (LG) muscles was evaluated. In isoflurane anesthetized animals, the sciatic nerve was exposed as it leaves the pelvis and two needle electrodes (Ambu #74325-36/40, Columbia, MD, United States) were placed in contact with it. Bipolar fine wire (Stablohm 800 A, California Fine Wire) electrodes (Basmajian & Stecko, 1963) were inserted transcutaneously into the centers of the TA and LG muscles using a 25G hypodermic needle. The free ends of the wires were connected to the head stages of differential amplifiers. Ongoing activity recorded from these muscles was sampled at 10 KHz by a laboratory computer system running custom Labview® software and when activity over a 10 ms period was within a user-defined background range, the computer delivered a single brief (0.3 ms) constant voltage pulse to the nerve via the needle electrodes and recorded EMG activity for 50 ms. In each animal, a range of stimulus intensities was applied, extending from subthreshold to supramaximal. To avoid fatigue, stimuli were delivered no more frequently than once every five seconds. Amplitudes of the

recorded direct muscle (M) responses were measured as the average full wave rectified voltage between the onset and duration of the recorded triphasic action potential. For each muscle tested in each mouse studied, the amplitude of the largest M response (Mmax) was determined.

Retrograde labeling experiments – The number of motor and sensory (dorsal root ganglion, DRG) neurons that successfully regenerated axons and reinnervated the TA and gastrocnemius (GAST) muscles was investigated using the application of retrograde fluorescent tracer molecules to these muscle targets, four weeks after bilateral sciatic nerve transection and repair, and two weeks after the cessation of daily treatments. This survival time was chosen to be compatible with those of previous studies (Al-Majed *et al.* , 2000b; English*et al.* , 2009; English *et al.* , 2011a; English *et al.* , 2011b; Udina *et al.* , 2011a; Gordon & English, 2016) evaluating activity-dependent experimental therapies to enhance peripheral axon regeneration. At the end of the electrophysiological experiments described above, the TA and gastrocnemius (GAST) muscles were exposed in the anesthetized animals. Two microliters of a 1% solution of wheat germ agglutinin (WGA), conjugated either to Alexa Fluor 488 (TA) or Alexa Fluor 555 (GAST), was injected into each muscle using a Hamilton microliter syringe equipped with a 36G needle. Small amounts of tracer were injected at two locations in each muscle and the needle was left in place for five minutes between injections to minimize leakage of the tracer along the needle track. After washing the entire surgical field three times with normal saline, surgical wounds were closed in layers before animals were returned to their cages. Three days later, the mice were euthanized by intraperitoneal injection of Euthasol and perfused transcardially with saline followed by 4% paraformaldehyde, pH 6.9. Lumbar spinal cords and L4 dorsal root ganglia (DRGs) were harvested and cryoprotected for at least 24 hours in 20% sucrose solution. Cryostat sections of spinal cords, in a horizontal plane at 40 μm thickness, were mounted onto charged slides and cover slipped using Vectashield®. Images of these sections at 20X magnification, using a Leica DM6000 upright fluorescence microscope, HC PL APO 0.70 NA objective, and Hamamatsu low-light camera, were made using HCImage software. Labeled motoneurons were identified if the retrograde fluorescence filled the soma and extended into the proximal dendrites and if a clear area of the cell corresponding to the nucleus could be visualized, as described previously (English, 2005). Profiles of motoneurons that did not meet these criteria were not counted. Harvested dorsal root ganglia were sectioned on a cryostat at 40 μm thickness, mounted onto charged slides and cover slipped using Vectashield®. Imaging of these sections was identical to that used for spinal cords, above. A DRG neuron was considered labeled if the fluorescent marker filled the entire soma and a clear nuclear region could be identified.

Cell cultures – Mouse lumbar dorsal root ganglion cells were harvested to assay neurite outgrowth after drug treatment. Mice were decapitated under isoflurane anesthesia. The entire vertebral column was removed and immediately placed on a cooled surface under a laminar flow hood. Individual ganglia (L1-L6) were dissected and pooled in a tube containing room temperature Hanks' Balanced Salt Solution (HBSS). Following ganglia collection, the HBSS was removed and a dispase-collagenase solution was added back to the tube, which was then placed in a 37@C bead bath for an hour-long incubation. During this one-hour period, the tube containing ganglia was briefly removed from the bead bath every 10 minutes and gently agitated by hand to ensure even enzymatic digestion of tissue. After incubation, dispase-collagenase was removed and replaced with DNase for 2.5 minutes. Then, without removing the DNase, pre-warmed (37@C) HBSS was added to the tube and tissue was further dissociated into a cell suspension by repeatedly pipetting with a P1000 pipet. The cell suspension was centrifuged at 1000 rcf for 3 minutes. The supernatant was subsequently discarded and the remaining pellet of cells was resuspended in Neurobasal A medium supplemented with B-27 (2%), GlutaMAX (1%), and penicillin-streptomycin (1%). Cells (3000/coverslip) were seeded directly onto laminin- and poly-D-lysine-coated 12 mm glass coverslips placed at the bottom of each well of a 4-well plate and the volume of media in each well was brought to 500 μL. Plates were stored in a water-jacketed incubator maintained at 37@C and steadily supplied with 5% CO_2. Twenty-four hours after plating, half of the media from each well was removed and replaced with fresh media with or without the drugs of interest. After allowing an additional 24 hours of incubation, cells were fixed in a solution of 4% paraformaldehyde in phosphate-buffered saline (PBS), then washed three times for five minutes in cold PBS, and stored in PBS at 4@C for up to a week before immunofluorescent antibody detection. Cultures used cells derived from both

WT mice and AEP knockout (KO) mice (Shirahama-Noda *et al.* , 2003). All mice used were genotyped from tail samples by Transnetyx, Inc. prior to use.

Immunofluorescence Staining of Cultured Neurons – Paraformaldehyde-fixed dorsal root ganglion cells attached to 12 mm glass coverslips were incubated with primary antibodies to protein targets (Table I), and then fluorescent secondary antibodies for detection (Table I). After blocking nonspecific binding and permeabilizing cells with a buffer (10% donkey serum and 0.3% Triton X-100 in PBS) at room temperature for one hour, primary antibodies were diluted in this same buffer, and the plate containing the cells was kept in continuous agitation at 4@C overnight. The following morning, cells were washed in PBS and then incubated with secondary antibodies in buffer at room temperature for two hours before washing again and mounting on glass slides with Vectashield with DAPI. Images of cells were captured at 20X magnification as described above. Neurite lengths were measured using the FIJI software package.

Statistical analyses – Numbers of animals in experimental groupings used were deemed adequate based on a post-hoc power analysis performed using G*Power 3.1 (Power = (1-β err prob) >0.8). All statistical comparisons were performed using GraphPad Prism software. If results of analyses of variance were significant,*post-hoc* paired testing using the two-stage linear step-up procedure of Benjamini, Krieger and Yekutieli was employed, unless noted otherwise. Alpha for significance of differences was set at $p<0.05$ throughout.

Results

CP11 treatments inhibit AEP activity at nerve injury sites – Asparaginyl endopeptidase activity was assayed at the site of sciatic nerve transection and repair at three and seven days after the start of treatments. Measures of activity at the two post-injury times from five nerves from WT mice treated with CP11 and five nerves from WT mice treated with vehicle, at two different times after injury, were compared to the activity measured in five intact nerves from control mice (Fig. 1). Results of a one-way ANOVA of these data were significant ($F_{4,\ 20} = 9.362$, p=0.0002). Based on the results of*post hoc* paired testing, AEP activity was increased significantly after nerve injury, relative to intact nerves, as was anticipated from the results of immunoblotting reported previously (English *et al.* , 2021). At both post-injury times studied, treatments with CP11 significantly reduced the magnitude of this increase in activity. After seven days of daily CP11 treatments, the reduction in AEP enzymatic activity was to a level that was not significantly different from that measured in the nerves of intact mice (Fig. 1).

CP11 treatments facilitate recovery of neuromuscular function – Compound muscle action potentials (M responses) were evoked in the LG and TA muscles by sciatic nerve stimulation four weeks after sciatic nerve transection and repair in mice treated for two weeks with either CP11 or vehicle (Fig. 2A). Examples of maximum M responses recorded from a vehicle-treated mouse and from a CP11-treated mouse four weeks after sciatic nerve transection and repair are shown in Figure 2B. Two types of treatments were evaluated: daily intraperitoneal (i.p.) injections and daily administration by oral gavage. For the mice receiving i.p injections, average Mmax amplitudes recorded in TA and LG from males and females were compared using a two-way (sex and treatment) analysis of variance (ANOVA). In these analyses, the effect of treatment was significant in both TA ($F_{1,20}$=6.630, p<0.0203) and LG ($F_{1,20}$=12.99, p=0.0018), but neither for sex (TA: $F_{1,20}$=0.186, p=0.671; LG: $F_{1,20}$=3.639, p=0.071), nor for the interaction of sex and treatment (TA: $F_{1,20}$=0.058, p=0.812; LG: $F_{1,20}$=3.114, p=0.0929). Data from males and females were combined for further analysis. We assumed that a similar lack of sex difference was present in the mice treated orally with CP11. We then evaluated the significance of differences between the two groups of CP11-treated mice and vehicle-treated mice for each muscle using a one-way ANOVA and *post hoc* paired tests, as appropriate. Results of the ANOVA were significant for both LG ($F_{3,\ 37} = 3.98$, p=0.0149) and TA ($F_{3,\ 37} = 4.567$, p=0.0081). For both muscles, both i.p. and oral administration of CP11 resulted in a significant increase in Mmax amplitude relative to identically administered vehicle treatments (Fig. 2C). Differences in Mmax amplitude between animals treated with CP11 via different routes of administration were not significant for both muscles. Four weeks after nerve injury, restoration of neuromuscular activity was improved more than twofold in mice treated with CP11, either orally or via i.p. injection, relative to vehicle-treated controls.

Axons of more motoneurons regenerate successfully after CP11 treatments – Following injection of the retrograde tracers WGA 555 into GAST and WGA 488 into TA, motoneurons were identified in horizontal sections of the lumbar spinal cord containing these fluorescent markers (Fig. 3A), indicating that their motor axons had regenerated and successfully reinnervated those muscles. A small number of motoneurons contained both retrograde tracers (Fig. 3A: yellow arrows), suggesting that their regenerating axons may have branched and were exposed to both tracers. As above, two different routes of administration of CP11 were used in different groups of mice. In the mice receiving CP11 or vehicle via i.p injections, we conducted a two-way (sex and treatment) ANOVA to evaluate if a sex difference existed. Results for both GAST and TA indicated a significant difference among treatment groups with regard to number of labeled motoneurons (TA: $F_{1,14}$=10.7, p<0.0075; GAST:$F_{1,14}$=136.00, p<0.0001), but not for sex (TA: $F_{1,14}$=0.059, p=0.813; GAST: $F_{1,14}$=0.045, p=0.835), or the interaction of sex and treatment (TA: $F_{1,14}$=4.766, p=0.0516; GAST: $F_{1,14}$=0.0018, p=0.967). We then combined the data from males and females and evaluated the significance of differences in numbers of retrogradely labeled motoneurons reinnervating TA, GAST or containing both tracers between CP11-treated (both oral and i.p injected) and vehicle-treated mice using a one-way ANOVA. Results were significant for GAST ($F_{3,\ 26}$ = 35.45, p<0.0001) and TA ($F_{3,\ 26}$ = 4.724, p=0.0140), but not for Both ($F_{3,\ 24}$ = 0.6285, p=0.6037). Using*post hoc* paired testing, the number of retrogradely labeled motoneurons encountered was significantly greater in mice treated with CP11 than in mice treated with vehicle for both GAST and TA. The number of labeled motoneurons in mice treated with CP11 via intraperitoneal injection was not significantly different from the number in mice treated via oral gavage (Fig. 3B). Both oral and injectable treatments with CP11 nearly doubled the number of motoneurons whose axons regenerated and successfully reinnervated the TA and GAST muscles while not changing the number of motoneurons whose axons were exposed to both retrograde tracers.

CP11 treatments enhance muscle sensory axon regeneration – The same protocol was used to evaluate the effects of CP11 treatments on motor axon regeneration and study the regeneration of sensory axons reinnervating the TA and GAST muscles (Fig. 4A). The numbers of retrogradely labeled neurons in L4 DRGs were compared in mice four weeks after transection and repair of the sciatic nerve and two weeks of treatment with either CP11 or vehicle. Mean (+ SEM) numbers of cells labeled from tracer injections into the different muscles and with different treatments are shown for mice treated with CP11 via intraperitoneal injection and from mice treated orally (Figure 4B). For each data set, a one-way ANOVA was conducted on these data and proved significant for TA and GAST, but not Both (TA: $F_{3,20}$= 7.588, p<0.001; GAST: $F_{3,\ 20}$ = 11.89, p=0.0001; Both: $F_{3,\ 20}$ = 1.445, p<0.2596). Applying *post hoc* paired testing, we found significantly more sensory neurons whose axons had regenerated and reinnervated the TA and GAST muscles in mice treated with CP11 than in mice treated with vehicle. Among the relatively small number of sensory neurons containing both retrograde labels, no significant difference was found between the vehicle-treated and CP11-treated animals.

CP11 treatments promote neurite elongation in cultured DRG cells – We cultured adult DRG neurons for 24 hours and then exposed the cells to different treatments for another 24 hours. To evaluate the effects of these treatments on neurite outgrowth, we measured the lengths of the longest neurites in each of at least 50 neurons per culture, identified by immunoreactivity to β3-tubulin, in cultures from six WT mice. In each well of a four-well plate, half of the initial plating media was removed and replaced with fresh media containing 7,8-DHF (500 nM), CP11 (5 uM), both 7,8-DHF and CP11, or no drug, termed Media. In the Media group, 0.02% DMSO was added, as this was the final concentration of DMSO in media containing diluted drug stocks. An example of a DRG neuron and the neurite measured from it is shown in Figure 5A. Cumulative frequency distributions of neurite lengths were constructed for each run in each of the four treatment groups and the data were fitted with a non-linear (Gaussian percentages) function. Fitted distributions for the six runs (cultures from different mice) were then averaged for each treatment group. These average frequency distributions are shown for the four groups by the solid lines in Figure 5B. The curves fitted to the frequency distributions for the cultures treated with CP11, 7,8-DHF, and the combined treatment are clearly shifted to the right of controls (Media), indicating that neurite lengths were increased by these treatments. Average median neurite lengths in each of these groups (Fig. 5C) were significantly longer than controls (ANOVA

$F_{3,\ 20} = 28.04$, $p<0.0001$). Using *post hoc* (Tukey) paired testing, average median neurite lengths were significantly longer in the cultures treated with 7,8-DHF, CP11, or 7,8-DHF and CP11 (Both) than those in the control cultures, but no significant difference in median length was found between neurites in the three groups of treated cultures. Treatments with either 7,8-DHF or CP11 enhance neurite length by the same amount. Combining the two treatments did not increase this enhancement.

Enhancement of neurite outgrowth produced by CP11 treatment is TrkB-independent – An additional set of cultures from WT mice was treated with CP11 or 7,8-DHF, as above, but some of the treated cultures also were exposed to the specific TrkB inhibitor, ANA-12. The distributions of neurite lengths measured in these cultures are shown in Figure 6A. Because the standard deviations of the groups compared were found to be significantly different, we performed a Brown-Forsythe ANOVA ($F_{5,\ 302.5} = 117.18$, $p<0.0001$) and Dunnett's T3 *post hoc* paired testing to evaluate the significance of differences in neurite lengths in the different culture conditions. Neurite lengths were increased significantly by exposure to CP11, relative to Media controls, whether or not the treatment also included ANA-12. As anticipated, a significant increase in neurite elongation produced by 7,8-DHF treatment alone was blocked completely by administration of ANA-12. Treatment of cultures with ANA-12 alone produced no significant effect on neurite length. Enhancement of neurite elongation produced by CP11 is thus TrkB-independent.

We also investigated whether the effects of CP11 treatments on neurite elongation were effective in cultured DRG neurons expressing or lacking the TrkB receptor. Cultures from wild type mice were treated as above and neurons were identified by immunoreactivity to ß3-tubulin to mark neurites. Cells were also reacted with an antibody to the extracellular domain of the TrkB receptor. For each neurite measured, the cell of origin was scored as $TrkB^+$ or $TrkB^-$. Examples of such cells are shown in Figure 6B. Five sets of cultures were studied. Neurite lengths measured in each culture were scaled to the average median neurite length in the untreated control cultures (Media). Results of these scaled neurite lengths from TrkB+ and TrkB- neurons in control, CP11-treated and 7,8-DHF-treated cultures are shown in Figure 6C as cumulative histograms. Average (+ SEM) median scaled neurite lengths are shown in Figure 6D. Significance of differences between groups was evaluated using ANOVA and post hoc paired testing. Treatments with CP11 or 7,8-DHF were equally effective in promoting outgrowth of neurites from $TrkB^+$ DRG neurons (Fig. 6C: Top), but only treatment with CP11 resulted in longer neurites in $TrkB^-$ neurons (Fig. 6C: Bottom).

Neurite outgrowth is enhanced in AEP knockout mice –Finally, we compared the elongation of neurites from neurons cultured from wild type (WT) mice to similar treatments in cultures from AEP knockout (AEP KO) mice (Shirahama-Noda *et al.* , 2003). All of the data from DRG neurons lacking AEP were compared to results of similar measurements from treated and untreated cultures from wild type mice. For analysis, all neurite lengths were scaled to the average median length of neurites measured in untreated cultures derived from WT mice. Results of a one-way ANOVA of these scaled neurite lengths were significant ($F_{5,\ 27} = 4.663$, $p=0.0034$). Using *post hoc* paired testing, neurite lengths in untreated DRG cells from AEP KO mice were significantly longer than those in cultures from untreated WT mice (Fig. 7). Lengths of neurites from neurons from AEP KO mice that had been treated with CP11 or 7,8-DHF also were significantly longer than those in the untreated cultures from wild type mice, but not significantly longer than neurites from untreated cells from AEP KO mice (Fig. 7). In the absence of AEP, neurite elongation was increased by about 50% over that observed in cells from WT mice without any treatment. This enhancement was not further increased by addition of the AEP inhibitor, CP11, or by treatment with 7,8-DHF. In addition, the lengths of neurites in all groups of DRG neurons from AEP KO mice were not significantly different from those of neurons derived from WT mice that had been exposed to either 7,8-DHF or CP11. Thus, inhibition of AEP by CP11 treatment resulted in an effect on neurite outgrowth similar to knocking out the AEP gene.

Discussion

Poor functional recovery from injuries to peripheral nerves is a significant public health issue. Such injuries are relatively common and despite the well-documented ability of axons to regenerate following PNI, they do so poorly. The successes of experimental treatments that promote axon regeneration after peripheral nerve injury in preclinical studies, such as exercise (Udina *et al.* , 2011a; English *et al.* , 2014) or electrical

stimulation (Al-Majed *et al.* , 2000b; Gordon & English, 2016) are dependent on signaling between BDNF and its TrkB receptor (Al-Majed *et al.* , 2000a; Wilhelm *et al.* , 2012). Treatments of mice with small molecule TrkB agonists or prodrugs that generate them also result in enhanced regeneration (English*et al.* , 2013; English *et al.* , 2022). We hypothesized that at least one target of all of these treatments is AEP. A prediction of this hypothesis is that downstream effectors of BDNF-TrkB signaling inhibit AEP, which then reduce or eliminate its cleavage of Tau and APP, and in doing so promote axon regeneration.

In the present study, we evaluated our hypothesis using a specific AEP inhibitor, compound 11 (CP11) (Zhang *et al.* , 2017). The main findings reported here are: 1) oral treatments with CP11 inhibit AEP activity at the site of nerve injury; and 2) systemic treatments with CP11 enhance motor and sensory axon regeneration after PNI. When administered either orally or by i.p. injection, CP11 treatments resulted in successful axon regeneration and muscle reinnervation by significantly more motor and sensory neurons than vehicle treated controls. Restoration of compound muscle action potentials (M wave amplitudes) was greater in CP11-treated mice than in controls. These findings are consistent with our hypothesis that inhibition of AEP is a prime target of experimental therapies for treating PNI, whether by activity-dependent or pharmacological approaches.

To begin to investigate the cellular mechanisms that might be involved, we compared the effects of treatment with 7,8-DHF and CP11 on neurite outgrowth from cultured DRG neurons. Both the small molecule TrkB ligand, 7,8-DHF, and the specific AEP inhibitor, CP11, significantly increased the growth of neurites when added individually to cultures but when added together they produced no significant increase over that observed when either was used alone. Similarly, addition of 7,8-DHF or CP11 to cultures from AEP-KO mice produced no significant effect on neurite outgrowth relative to untreated cultures of DRG neurons from the same animals. The extent of enhancement of neurite outgrowth in these cultures also was not significantly different from the effects of treatments with 7,8-DHF, CP11, or both on the lengths of neurites from neurons derived from WT mice. These outcomes all are consistent with our hypothesis that the effectiveness of treatments that enhance axon regeneration by stimulating TrkB activation, such as treatments with 7,8-DHF (English *et al.* , 2013) or prodrugs (English *et al.* , 2022), as well as activity-dependent experimental therapies that increase BDNF and/or TrkB expression in rats (Al-Majed *et al.* , 2000a) and mice (Wilhelm *et al.* , 2012), all do so primarily by inhibiting AEP. Activation of the TrkB receptor in these scenarios results in its phosphorylation and a downstream inhibition of AEP, leading to a decrease in cleavage of the microtubule domain of Tau at asparagine 368 and a promotion of axon regeneration (English *et al.* , 2021). A similar effect is achieved by direct AEP inhibition via CP11 treatments.

Of particular interest were the results of experiments in which the effects of the treatments were evaluated in cells that expressed the TrkB receptor. Treatments with CP11 stimulated neurite outgrowth in all cells, regardless of phenotype, but, as might be predicted, treatments with 7,8-DHF were effective only in neurons that expressed the TrkB receptor. The mRNA for TrkB is widely expressed in alpha, but not gamma motoneurons in rats (Buck *et al.* , 2000; Copray & Kernell, 2000). The robust effects of treatments with 7,8-DHF or its prodrug, R13, and the results presented here using CP11, on the regeneration of motor axons or/and restoration of M wave amplitude in reinnervated muscles are likely due to similar TrkB expression in mouse motoneurons. The regeneration of axons of a subset of sensory neurons that express the TrkB receptor, even as modified following PNI in rats (Karchewski*et al.* , 2002) or mice (English *et al.* , 2007), also would be expected to respond. However, sensory neurons not expressing TrkB would not benefit from such a TrkB-dependent therapy. We believe that these results suggest that direct AEP inhibition, such as that produced by CP11, might be overall the most effective therapy for PNI to date. This assertion does not discount the possibility that pathways alternative to the BDNF-TrkB pathway that result in inhibition of AEP may exist. Whether they are in play when activity-dependent treatments are employed remains for future study.

Conclusion: Inhibition of AEP activity is the main focus of activity-dependent and BDNF-TrkB dependent experimental therapies for peripheral nerve injury. Direct inhibition of AEP by CP11 is a potential treatment worthy of further consideration.

Table I

Antibodies Used

Target	Primary Antibody	Secondary Antibody	Dilution
ß3-tubulin	Cell Signaling #4466	donkey anti-mouse IgG/Alexa Fluor 488 or 594	1:250
TrkB	R&D Systems #AF1494	donkey anti-goat IgG/Alexa Fluor 647	1:20

Figure legends

Figure 1. Compound 11 treatment reduces AEP activity in injured nerves. Sciatic nerves were cut and surgically repaired in wild type mice. Beginning on the third post-injury day, animals were administered either CP11 or vehicle, orally, once daily. Repaired nerves were harvested and assayed for AEP activity on the third (3d) or seventh (7d) after the onset of treatment. A set of intact nerves was assayed similarly for controls. Mean (+ SEM) AEP activity is scaled to the maximum activity found in all samples.

Figure 2. Treatments with CP11 result in larger restored neuromuscular responses. A. Outline of experimental scheme. Mice were treated with CP11 or vehicle daily, five days per week for two weeks, beginning on the third day following sciatic nerve transection and repair. After two more weeks, neuromuscular reinnervation was tested. B. Examples of maximal amplitude M responses (Mmax) recorded four weeks after sciatic nerve transection and repair from a vehicle-treated (top) and a CP11-treated (bottom) mouse. C. Mean (+ SEM) amplitudes of Mmax recorded from tibialis anterior (TA) and lateral gastrocnemius (LG) in vehicle-treated and CP11-treated mice, either via i.p. injection or oral gavage, four weeks after sciatic nerve transection and repair. Significance of differences between CP11-treated and vehicle-treated mice was evaluated for each muscle using ANOVA and post hoc paired testing. P values are shown to indicate the significance of differences in paired comparisons.

Figure 3. Treatments with CP11 increase the number of motoneurons whose axons have regenerated successfully. A. Image of a horizontal section through the right side of the lumbar spinal cord of a mouse in which the sciatic nerve was cut and repaired four weeks earlier. Motoneurons were labeled by application of different fluorescent retrograde tracers into the reinnervated gastrocnemius (GAST, red) and tibialis anterior (TA, green) muscles. Three neurons in this image contained both tracers (yellow arrows). This mouse was treated with intraperitoneal injections of CP11. B. Mean (+ SEM) number of motoneurons retrogradely labeled from tracer injection into GAST and TA four weeks after sciatic nerve transection and repair and two weeks after treatment, either by intraperitoneal injection (i.p.) or orally (oral), with compound 11 (CP11, 10 mg/Kg), or vehicle. Numeric values indicate p values from pairwise comparisons (ns = not significant).

Figure 4. Treatments with compound 11 (CP11) increased the number of muscle sensory neurons whose axons regenerated successfully. A. In a section from the L4 DRG of a mouse four weeks after sciatic nerve transection and repair and two weeks after treatment with CP11, neurons retrogradely labeled from tracer injections into GAST (red) and TA (green) are shown. Three cells in this image were labeled by both tracers (yellow arrows). B. Mean (+ SEM) numbers of L4 DRG neurons retrogradely labeled from TA, GAST, or Both in vehicle-treated and CP11-treated mice are shown. Each symbol in each graph represents the number of labeled neurons in a single animal in the series. Significance of differences between groups are displayed as p values above comparison brackets.

Figure 5. Neurite elongation is enhanced by CP11 treatments. A. Example of an adult DRG neuron after 48 hours in culture, marked by immunoreactivity to β3 tubulin. This culture was treated for 24 hours with CP11. The arrows indicate the longest neurite measured in this cell. B. Cumulative frequency distributions of neurite lengths in four treatment groups. Each cumulative histogram represents the average of the distributions of neurite lengths from cultures of DRG neurons from six mice. The horizontal dashed line at the 50^{th}percentile marks the median neurite length, shown at the vertical dashed lines extending to the X axis. C. Average (+ SEM) median neurite lengths in six cultures of the four treatment groups.

Each symbol represents the neurite length measured from cells derived from a single animal. P values are shown only for significant differences between groups. All other paired comparisons were not statistically significant.

Figure 6. Enhancement of neurite outgrowth produced by CP11 treatment is TrkB-independent. A. Distributions of neurite lengths of cultured DRG neurons without treatments (Media) and after treatments with CP11 or 7,8-DHF in the presence or absence of the TrkB inhibitor, ANA-12 are displayed as violin plots. The solid white lines in each violin mark their medians. The horizontal dashed line running through the figure marks the median neurite length from the control group (Media). Numbers above brackets indicate p values associated with statistical comparisons between groups. B. Image of two β3 tubulin-immunoreactive DRG neurons (red) in a culture treated for 24 hours with CP11. Cultures also were reacted with an antibody to the extracellular domain of the TrkB receptor, and a green fluorescing secondary antibody. The lower cell in the image was scored as $TrkB^+$ and the upper cell as $TrkB^-$. C. Cumulative frequency distributions of neurite lengths in cultured adult DRG neurons identified as $TrkB^+$ (top) and $TrkB^-$ (bottom) in control (Media) cultures and in cultures treated with either CP11 or 7,8-DHF. Neurite lengths in cultures from different mice were scaled to the median neurite length in the corresponding control (Media only) group. Each cumulative histogram represents the average of the distributions of these scaled neurite lengths from cultures of DRG neurons from six mice. Medians for each group are represented by the projection of the dashed line at the 50^{th} percentile to the horizontal. D. Average (+ SEM) median scaled neurite lengths from the same cultures are shown for TrkB+ (top) and TrkB- (bottom) neurons. Numbers above brackets are p values resulting from statistical comparisons made between groups.

Figure 7. Neurite length is not increased by CP11 treatments in AEP knockout mice. Average median neurite lengths (+ SEM), scaled to the median length found in untreated cultures derived from WT mice, are shown for cultures from AEP KO mice and those derived from WT mice. Data from untreated cultures (Media), cultures treated with CP11 (red bars), cultures treated with 7,8-DHF (green bars) are shown. Numbers above brackets indicate p values for all significant differences between groups. All other paired comparisons were not statistically significant.

References

Akhter, E.T., Rotterman, T.M., English, A.W. & Alvarez, F.J. (2019) Sciatic nerve cut and repair using fibrin glue in adult mice. *Bio Protoc* , **9** , e3363.

Al-Majed, A.A., Brushart, T.M. & Gordon, T. (2000a) Electrical stimulation accelerates and increases expression of BDNF and trkB mRNA in regenerating rat femoral motoneurons. *Eur J Neurosci* ,**12** , 4381-4390.

Al-Majed, A.A., Neumann, C.M., Brushart, T.M. & Gordon, T. (2000b) Brief electrical stimulation promotes the speed and accuracy of motor axonal regeneration. *J Neurosci.* , **20** , 2602-2608.

Al-Majed, A.A., Tam, S.L. & Gordon, T. (2004) Electrical stimulation accelerates and enhances expression of regeneration-associated genes in regenerating rat femoral motoneurons. *Cell Mol Neurobiol* ,**24** , 379-402.

Basmajian, J.V. & Stecko, G. (1963) The role of muscles in arch support of the foot. *J Bone Joint Surg Am* , **45** , 1184-1190.

Bekelis, K., Missios, S. & Spinner, R.J. (2015) Falls and peripheral nerve injuries: an age-dependent relationship. *J Neurosurg* ,**123** , 1223-1229.

Boeltz, T., Ireland, M., Mathis, K., Nicolini, J., Poplavski, K., Rose, S.J., Wilson, E. & English, A.W. (2013) Effects of treadmill training on functional recovery following peripheral nerve injury in rats.*J Neurophysiol* , **109** , 2645-2657.

Buck, C.R., Seburn, K.L. & Cope, T.C. (2000) Neurotrophin expression by spinal motoneurons in adult and developing rats. *J. Comp. Neurol.* , **416** , 309-318.

Copray, S. & Kernell, D. (2000) Neurotrophins and trk-receptors in adult rat spinal motoneurons: differences related to cell size but not to 'slow/fast' specialization. *Neurosci. Let.* , **289** , 217-220.

English, A.W. (2005) Enhancing axon regeneration in peripheral nerves also increases functionally inappropriate reinnervation of targets.*J Comp Neurol* , **490** , 427-441.

English, A.W., Carrasco, D., Hoffman, D., Isaacson, R., Kang, S.S., Khan, S., Liu, X. & Ye, K. (2022) Oral Treatments With the TrkB Ligand Prodrug, R13, Promote Enhanced Axon Regeneration Following Peripheral Nerve Injury. *Frontiers in Cellular Neuroscience* , **16** .

English, A.W., Cucoranu, D., Mulligan, A., Rodriguez, J.A. & Sabatier, M.J. (2011a) Neurotrophin-4/5 is implicated in the enhancement of axon regeneration produced by treadmill training following peripheral nerve injury. *Eur J Neurosci* , **33** , 2265-2271.

English, A.W., Liu, K., Nicolini, J.M., Mulligan, A.M. & Ye, K. (2013) Small-molecule trkB agonists promote axon regeneration in cut peripheral nerves. *Proceedings of the National Academy of Sciences* ,**110** , 16217-16222.

English, A.W., Liu, X., Mistretta, O.C., Ward, P.J. & Ye, K. (2021) Asparagine Endopeptidase (delta secretase), an enzyme implicated in Alzheimer's disease pathology, is an inhibitor of axon regeneration in peripheral nerves. *eNeuro* , **8** .

English, A.W., Mulligan, A., Cucoranu, D. & Sabatier, M.J. (2009) Treadmill training enhances axon regeneration in cut peripheral nerves without effecting topographic specificity of reinnervating motoneurons.*J Comp Neurol* , **517** , 245-255.

English, A.W., Mulligan, A., Meador, W., Sabatier, M.J. & Schwartz, G. (2007) Electrical stimulation promotes peripheral axon regeneration by enhanced neuronal neurotrophin signaling. *Dev. Neurobiol.* ,**67** , 158-172.

English, A.W., Wilhelm, J.C. & Sabatier, M.J. (2011b) Enhancing recovery from peripheral nerve injury using treadmill training.*Ann. Anat.* , **193** , 354-361.

English, A.W., Wilhelm, J.C. & Ward, P.J. (2014) Exercise, neurotrophins, and axon regeneration in the PNS. *Physiology* ,**29** , 437-445.

Gordon, T. & English, A.W. (2016) Strategies to promote peripheral nerve regeneration: electrical stimulation and/or exercise. *Eur J Neurosci* , **43** , 336-350.

Karchewski, L.A., Gratto, K.A., Wetmore, C. & Verge, V.M. (2002) Dynamic patterns of BDNF expression in injured sensory neurons: differential modulation by NGF and NT-3. *Eur J Neurosci* ,**16** , 1449-1462.

Scholz, T., Krichevsky, A., Sumarto, A., Jaffurs, D., Wirth, G., Paydar, K. & Evans, G. (2009) Peripheral nerve injuries: An internationalsurvey of current treatments and future perspectives. *J Reconstr Microsurg* , **25** , 339-344.

Shirahama-Noda, K., Yamamoto, A., Sugihara, K., Hashimoto, N., Asano, M., Nishimura, M. & Hara-Nishimura, I. (2003) Biosynthetic processing of cathepsins and lysosomal degradation are abolished in asparaginyl endopeptidase-deficient mice. *J Biol Chem* , **278** , 33194-33199.

Udina, E., Cobianchi, S., Allodi, I. & Navarro, X. (2011a) Effects of activity-dependent strategies on regeneration and plasticity after peripheral nerve injuries. *Ann Anat* , **193** , 347-353.

Udina, E., Puigdemasa, A. & Navarro, X. (2011b) Passive and active exercise improve regeneration and muscle reinnervation after peripheral nerve injury in the rat. *Muscle & Nerve* , **43** , 500-509.

Wang, Z.H., Wu, W., Kang, S.S., Liu, X., Wu, Z., Peng, J., Yu, S.P., Manfredsson, F.P., Sandoval, I.M., Liu, X., Wang, J.Z. & Ye, K. (2018) BDNF inhibits neurodegenerative disease-associated asparaginyl endopeptidase activity via phosphorylation by AKT. *JCI Insight* ,**3** .

Wilhelm, J.C., Xu, M., Cucoranu, D., Chmielewski, S., Holmes, T., Lau, K., Bassell, G.J. & English, A.W. (2012) Cooperative roles of BDNF expression in neurons and Schwann cells are modulated by exercise to facilitate nerve regeneration. *Journal of Neuroscience* ,**32** , 5002-5009.

Zhang, Z., Obianyo, O., Dall, E., Du, Y., Fu, H., Liu, X., Kang, S.S., Song, M., Yu, S.P., Cabrele, C., Schubert, M., Li, X., Wang, J.Z., Brandstetter, H. & Ye, K. (2017) Inhibition of delta-secretase improves cognitive functions in mouse models of Alzheimer's disease. *Nature communications* , **8** , 14740.

Zhang, Z., Song, M., Liu, X., Kang, S.S., Kwon, I.S., Duong, D.M., Seyfried, N.T., Hu, W.T., Liu, Z., Wang, J.Z., Cheng, L., Sun, Y.E., Yu, S.P., Levey, A.I. & Ye, K. (2014) Cleavage of tau by asparagine endopeptidase mediates the neurofibrillary pathology in Alzheimer's disease. *Nat Med* , **20** , 1254-1262.

Zhang, Z., Song, M., Liu, X., Su Kang, S., Duong, D.M., Seyfried, N.T., Cao, X., Cheng, L., Sun, Y.E., Ping Yu, S., Jia, J., Levey, A.I. & Ye, K. (2015) Delta-secretase cleaves amyloid precursor protein and regulates the pathogenesis in Alzheimer's disease. *Nature communications* , **6** , 8762.

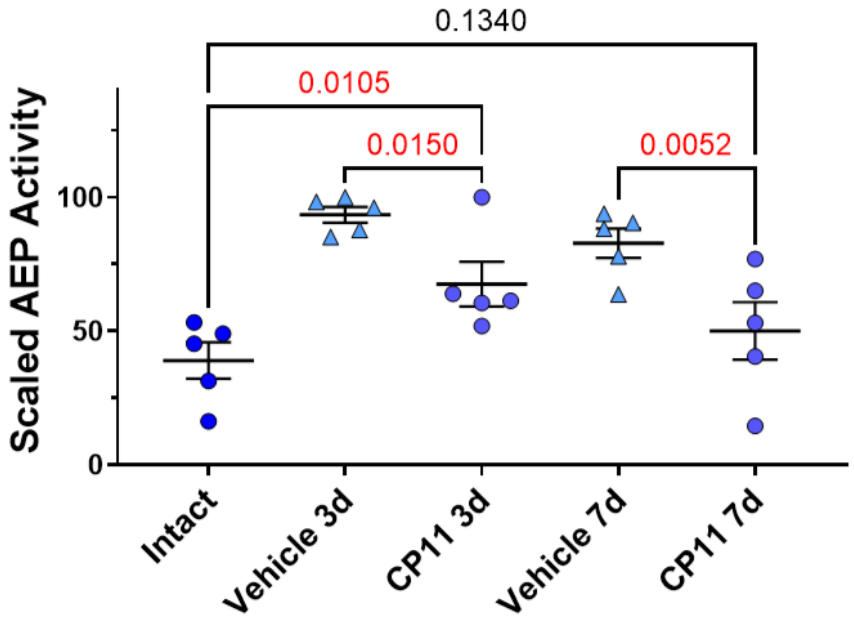

Figure 1. Compound 11 treatment reduces AEP activity in injured nerves. Sciatic nerves were cut and surgically repaired in wild type mice. Beginning on the third post-injury day, animals were administered either CP11 or vehicle, orally, once daily. Repaired nerves were harvested and assayed for AEP activity on the third (3d) or seventh (7d) after the onset of treatment. A set of intact nerves was assayed similarly for controls. Mean (+ SEM) AEP activity is scaled to the maximum activity found in all samples.

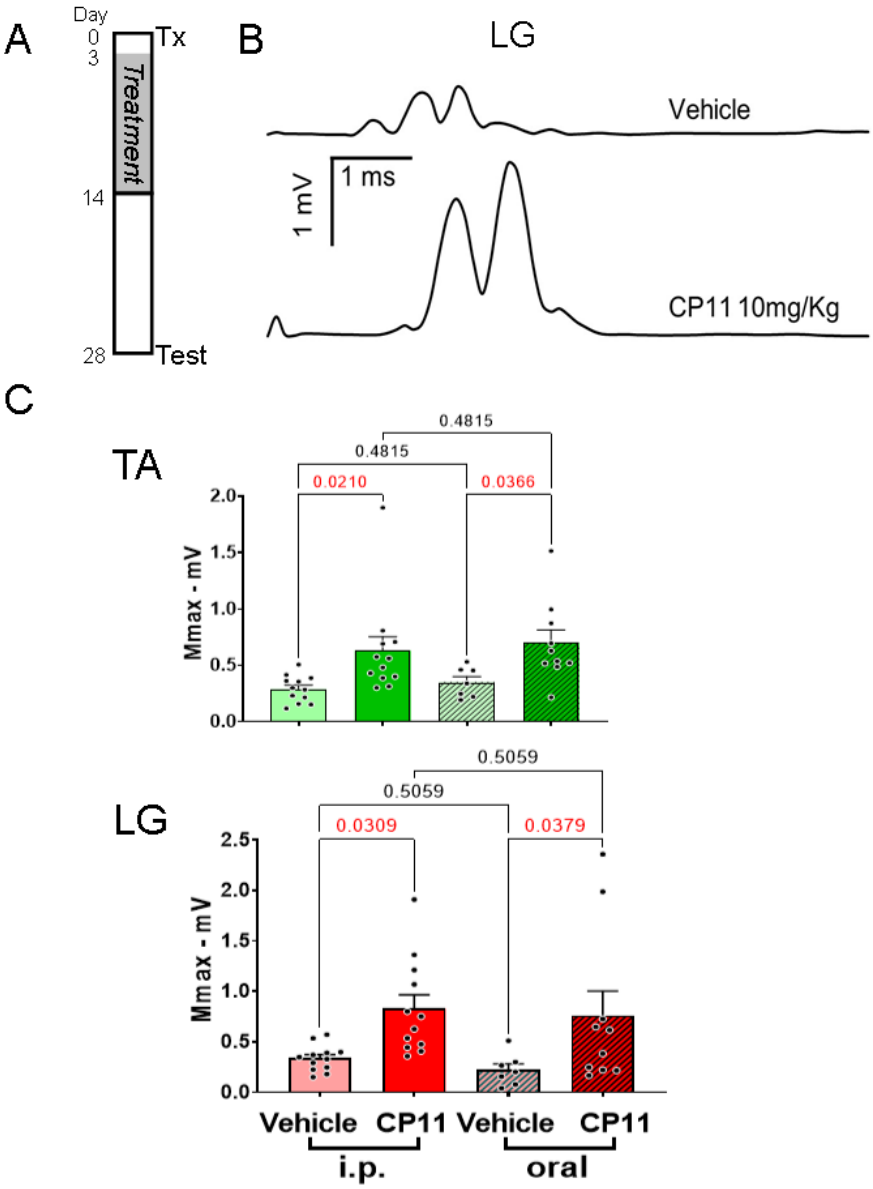

Figure 2. Treatments with CP11 result in larger restored neuromuscular responses. A. Outline of experimental scheme. Mice were treated with CP11 or vehicle daily, five days per week for two weeks, beginning on the third day following sciatic nerve transection and repair. After two more weeks, neuromuscular reinnervation was tested. B. Examples of maximal amplitude M responses (Mmax) recorded four weeks after sciatic nerve transection and repair from a vehicle-treated (top) and a CP11-treated (bottom) mouse. C. Mean (+ SEM) amplitudes of Mmax recorded from tibialis anterior (TA) and lateral gastrocnemius (LG) in vehicle-treated and CP11-treated mice, either via i.p. injection or oral gavage, four weeks after sciatic nerve transection and repair. Significance of differences between CP11-treated and vehicle-treated mice was evaluated for each muscle using ANOVA and post hoc paired testing. P values are shown to indicate the significance of differences in paired comparisons.

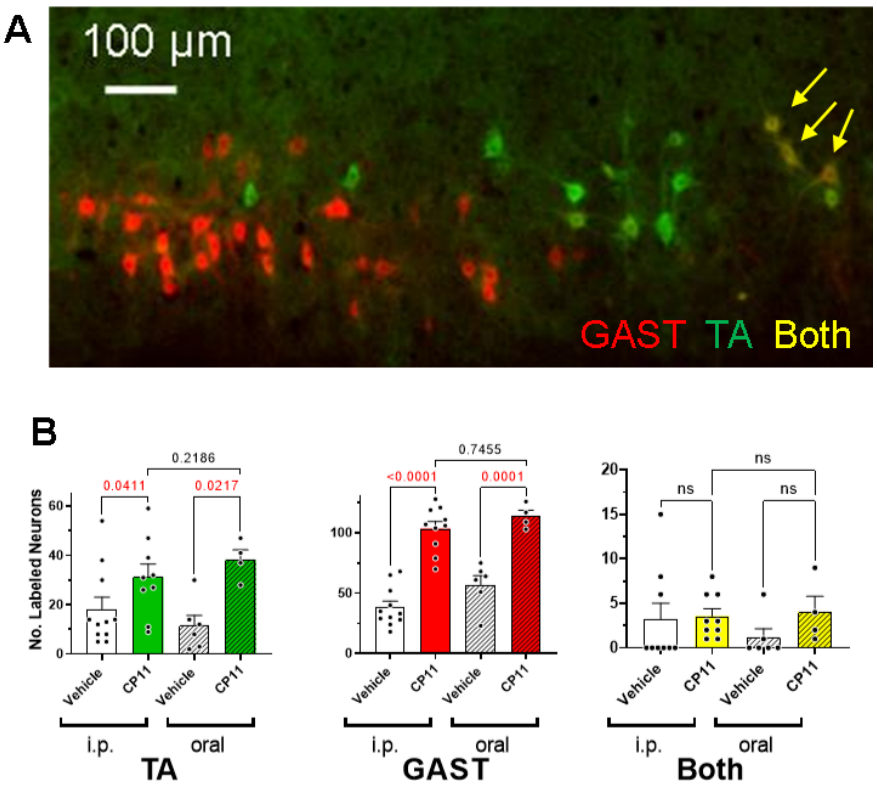

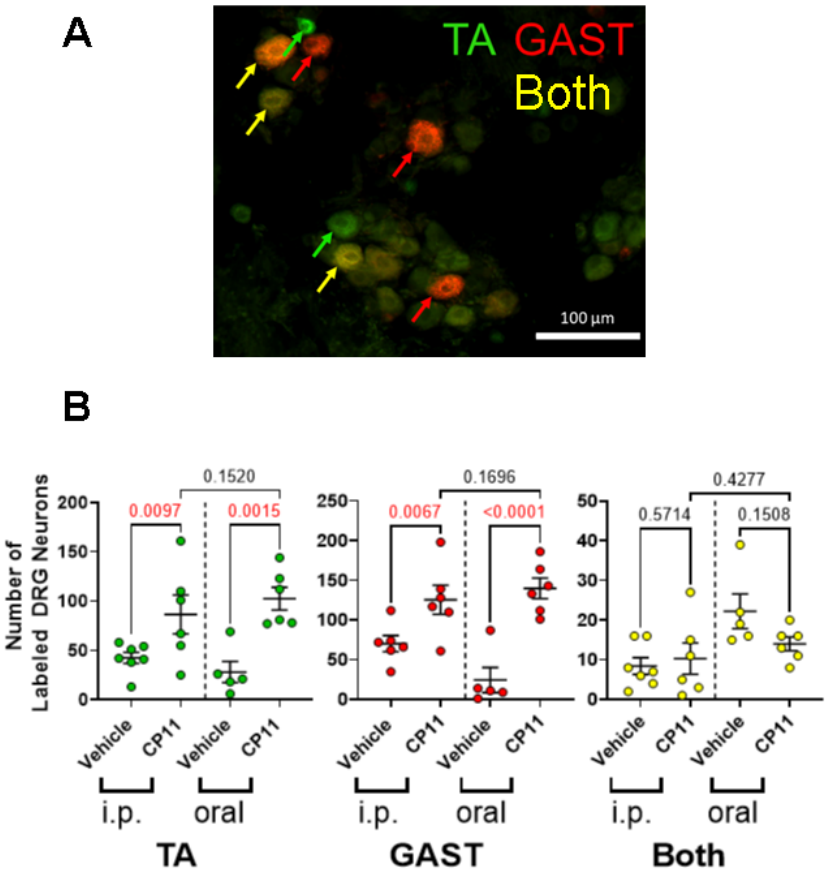

Figure 3. Treatments with CP11 increase the number of motoneurons whose axons have regenerated successfully. A. Image of a horizontal section through the right side of the lumbar spinal cord of a mouse in which the sciatic nerve was cut and repaired four weeks earlier. Motoneurons were labeled by application of different fluorescent retrograde tracers into the reinnervated gastrocnemius (GAST, red) and tibialis anterior (TA, green) muscles. Three neurons in this image contained both tracers (yellow arrows). This mouse was treated with intraperitoneal injections of CP11. B. Mean (+ SEM) number of motoneurons retrogradely labeled from tracer injection into GAST and TA four weeks after sciatic nerve transection and repair and two weeks after treatment, either by intraperitoneal injection (i.p.) or orally (oral), with compound 11 (CP11, 10 mg/Kg), or vehicle. Numeric values indicate p values from pairwise comparisons (ns = not significant).

Figure 4. Treatments with compound 11 (CP11) increased the number of muscle sensory neurons whose axons regenerated successfully. A. In a section from the L4 DRG of a mouse four weeks after sciatic nerve transection and repair and two weeks after treatment with CP11, neurons retrogradely labeled from tracer injections into GAST (red) and TA (green) are shown. Three cells in this image were labeled by both tracers (yellow arrows). B. Mean (+ SEM) numbers of L4 DRG neurons retrogradely labeled from TA, GAST, or Both in vehicle-treated and CP11-treated mice are shown. Each symbol in each graph represents the number of labeled neurons in a single animal in the series. Significance of differences between groups are displayed as p values above comparison brackets.

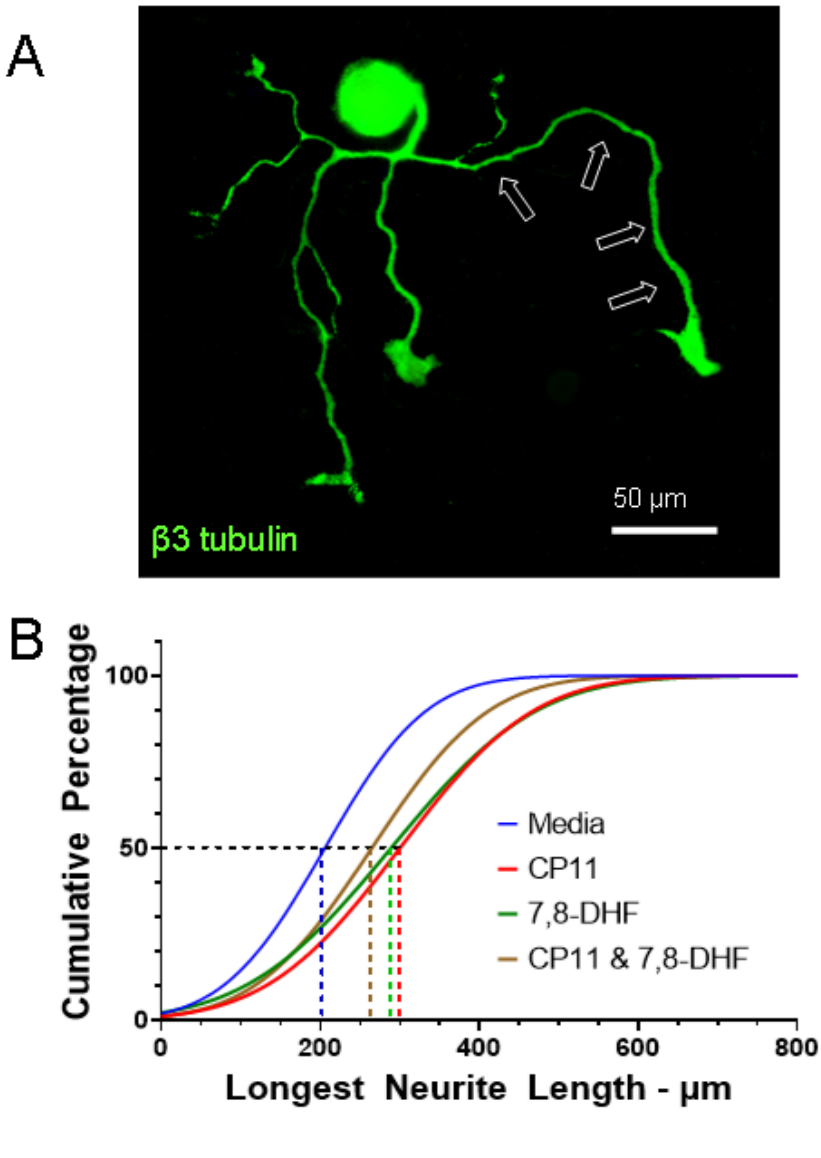

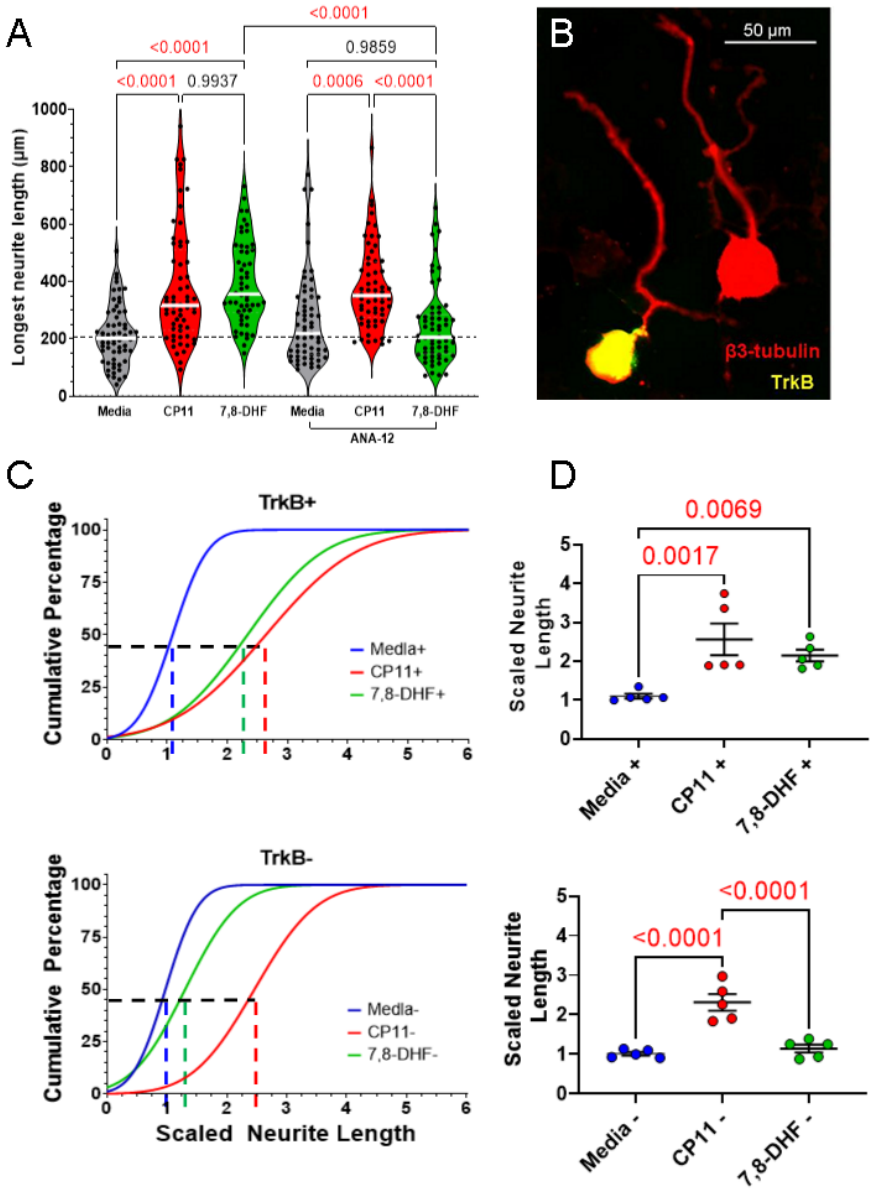

Figure 6 . Enhancement of neurite outgrowth produced by CP11 treatment is TrkB-independent. A. Distributions of neurite lengths of cultured DRG neurons without treatments (Media) and after treatments with CP11 or 7,8-DHF in the presence or absence of the TrkB inhibitor, ANA-12 are displayed as violin plots. The solid white lines in each violin mark their medians. The horizontal dashed line running through the figure marks the median neurite length from the control group (Media). Numbers above brackets indicate p values associated with statistical comparisons between groups. B. Image of two β3 tubulin-immunoreactive DRG neurons (red) in a culture treated for 24 hours with CP11. Cultures also were reacted with an antibody to the extracellular domain of the TrkB receptor, and a green fluorescing secondary antibody. The lower cell in the image was scored as TrkB+ and the upper cell as TrkB-. C. Cumulative frequency distributions of neurite lengths in cultured adult DRG neurons identified as TrkB+ (top) and TrkB- (bottom) in control (Media) cultures and in cultures treated with either CP11 or 7,8-DHF. Neurite lengths in cultures from different mice were scaled to the median neurite length in the corresponding control (Media only) group.

Each cumulative histogram represents the average of the distributions of these scaled neurite lengths from cultures of DRG neurons from six mice. Medians for each group are represented by the projection of the dashed line at the 50th percentile to the horizontal. D. Average (+SEM) median scaled neurite lengths from the same cultures are shown for TrkB+ (top) and TrkB- (bottom) neurons. Numbers above brackets are p values resulting from statistical comparisons made between groups.

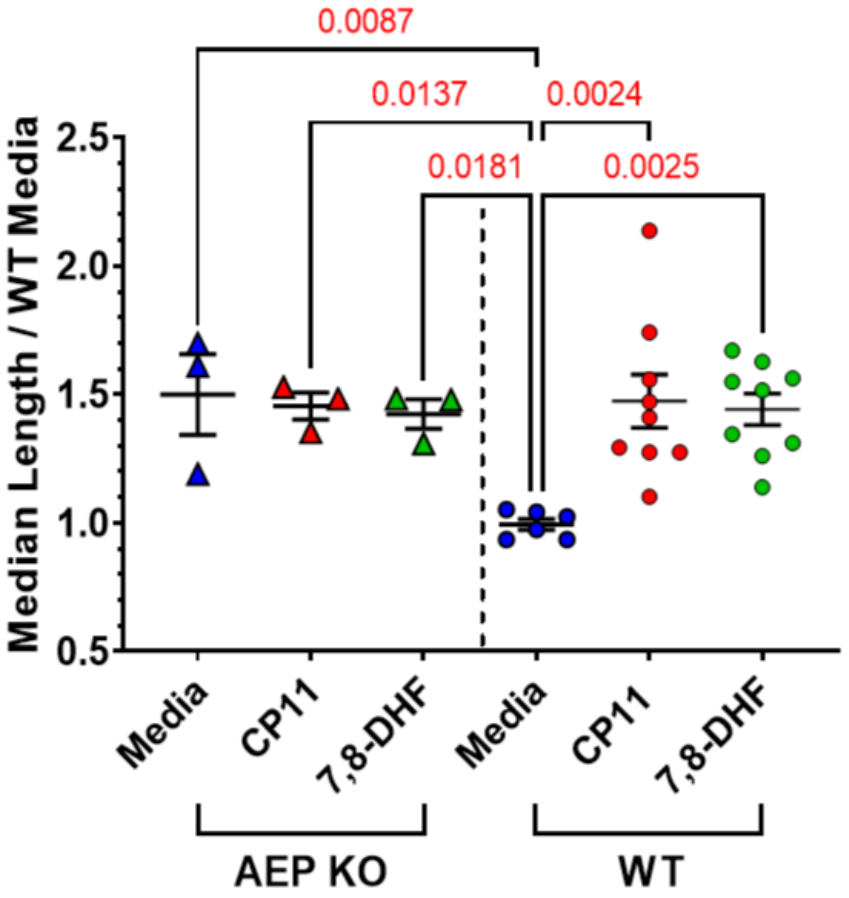

Figure 7. Neurite length is not increased by CP11 treatments in AEP knockout mice. Average median neurite lengths (+ SEM), scaled to the median length found in untreated cultures derived from WT mice, are shown for cultures from AEP KO mice and those derived from WT mice. Data from untreated cultures (Media), cultures treated with CP11 (red bars), cultures treated with 7,8-DHF (green bars) are shown. Numbers above brackets indicate p values for all significant differences between groups. All other paired comparisons were not statistically significant.

Graphical abstract

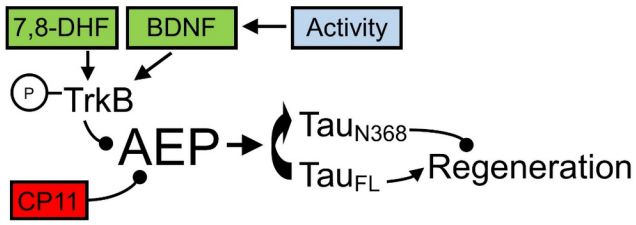

Increased activity of injured neurons promotes expression of BDNF which, acting via phosphorylation of the TrkB receptor, inhibits asparaginyl endopeptidase (AEP, δ-secretase), reducing cleavage of the microtubule associated protein Tau (Tau_{FL}) to Tau_{N368} an effect that hinders axon regeneration. Treatment with the TrkB agonist, 7,8-DHF acts similarly. Both approaches are bypassed by direct AEP inhibition via compound 11 (CP11).

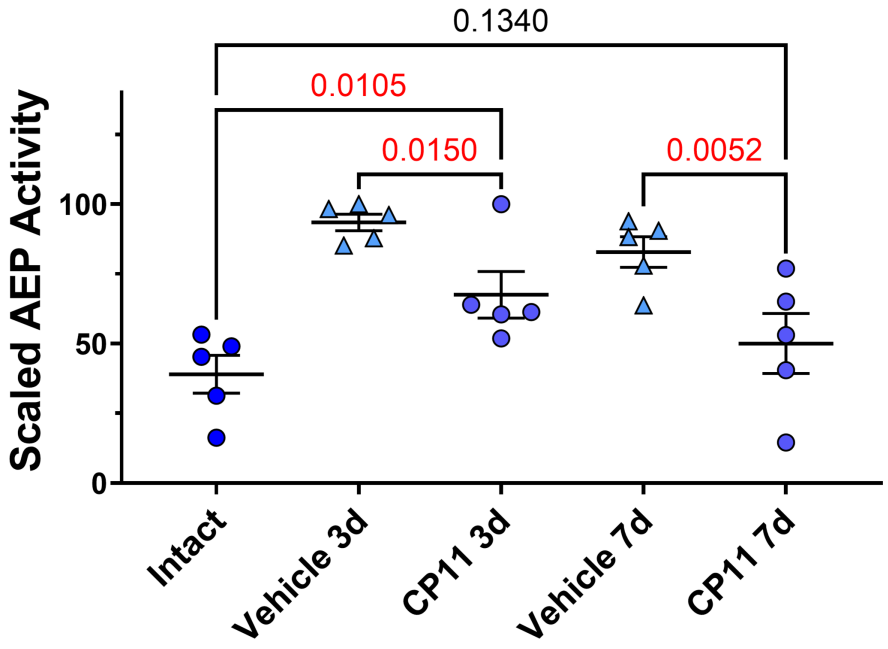

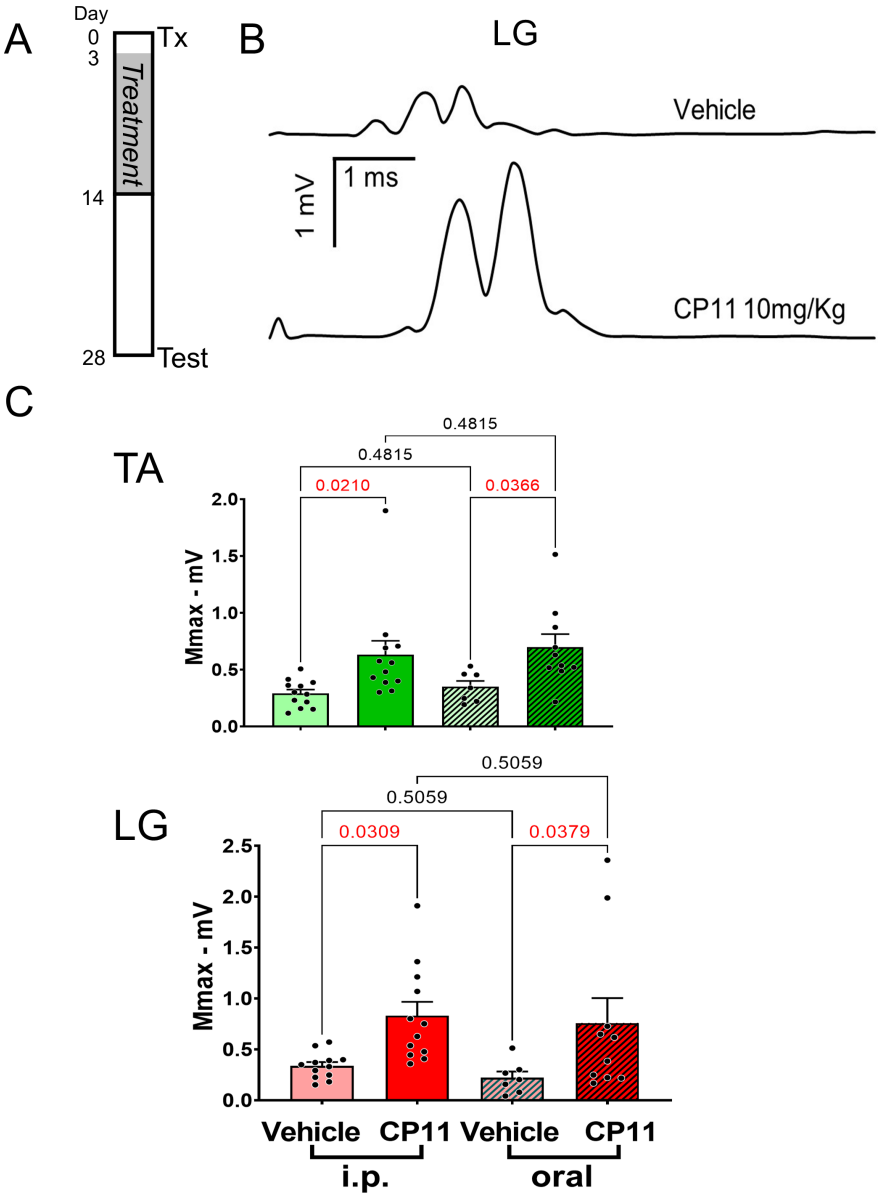

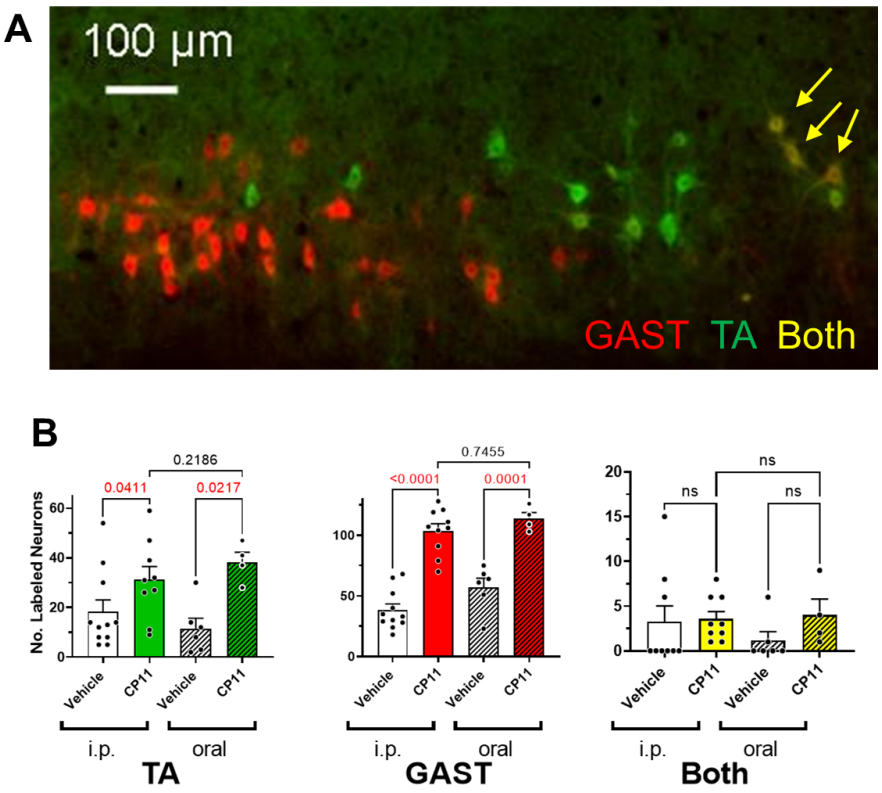

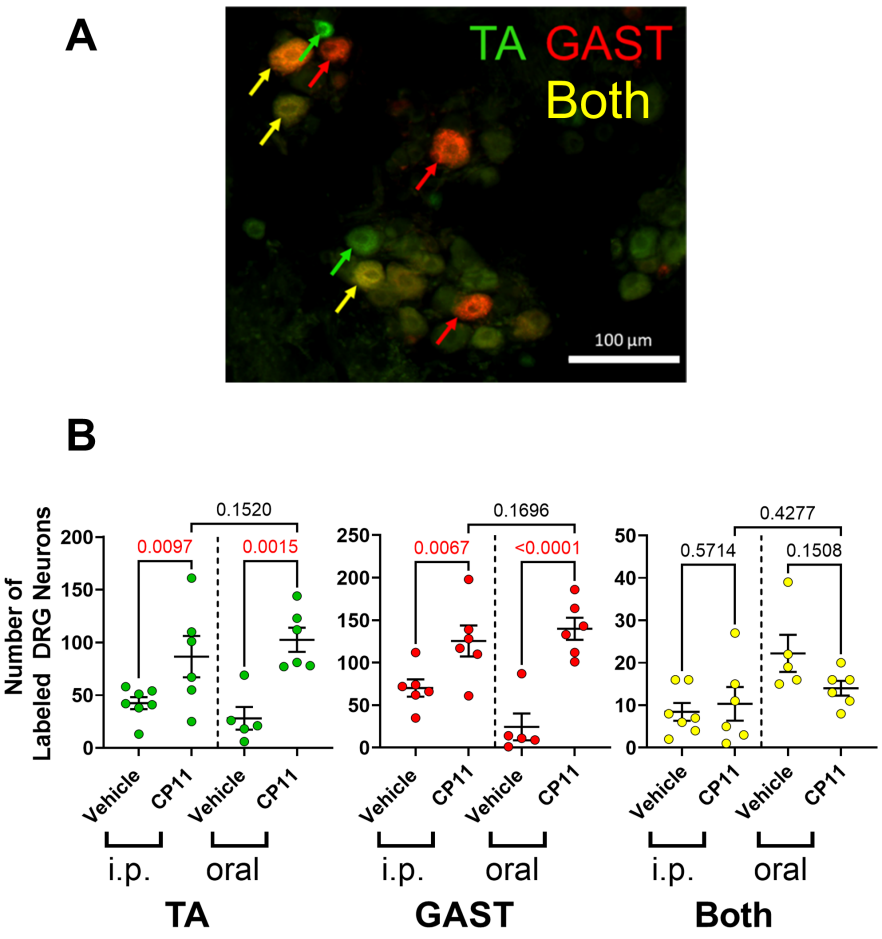

A

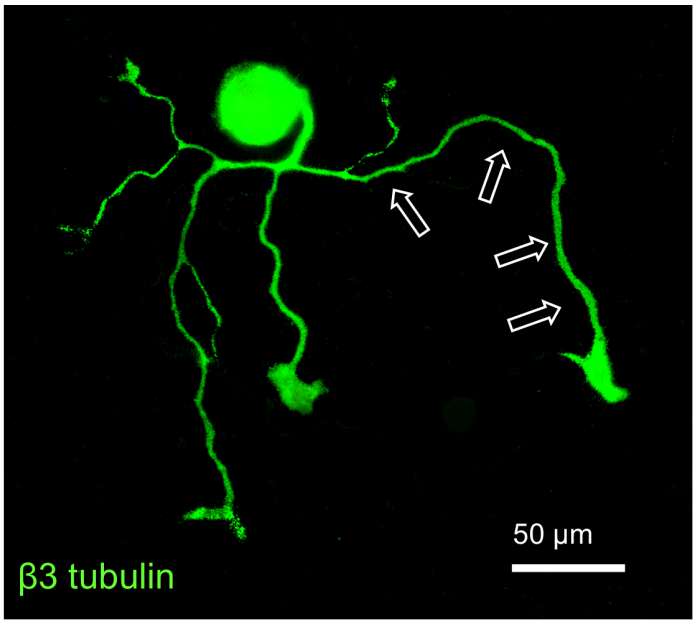

B

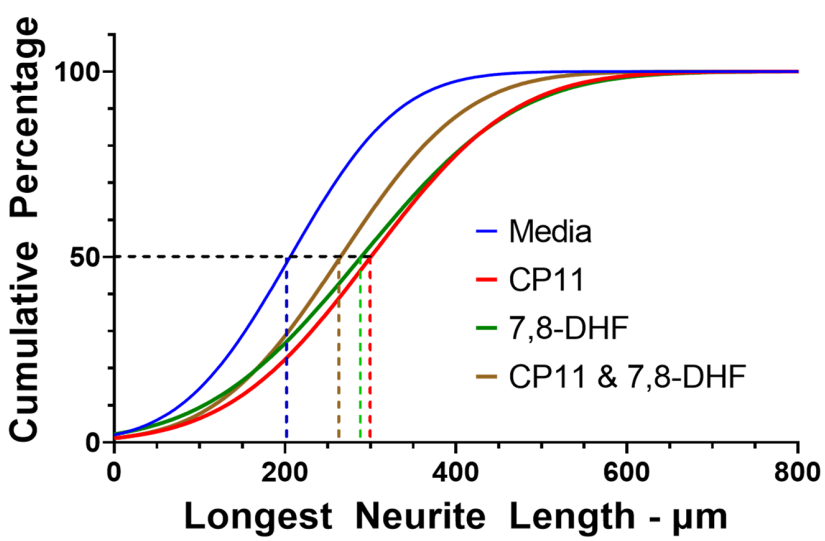

C